Journal of
Cardiovascular Imaging

JCVI

Review Article

Check for updates

Multimodality Imaging for the Assessment of Severe Aortic Stenosis

Sung-Ji Park iD**, MD, PhD[1] and Marc R. Dweck** iD**, MD[2]**

[1]Division of Cardiology, Department of Internal Medicine, Cardiovascular Imaging Center, Heart Vascular Stroke Institute, Samsung Medical Center, Sungkyunkwan University School of Medicine, Seoul, Korea
[2]British Heart Foundation Centre for Cardiovascular Science, University of Edinburgh, Edinburgh, Scotland, UK

OPEN ACCESS

Address for Correspondence:
Sung-Ji Park, MD, PhD
Division of Cardiology, Department of Medicine, Cardiovascular Imaging Center, Heart Vascular Stroke Institute, Samsung Medical Center, Sungkyunkwan University School of Medicine, 81 Irwon-ro, Gangnam-gu, Seoul 06351, Korea.
E-mail: tyche.park@gmail.com

ORCID iDs
Sung-Ji Park iD
https://orcid.org/0000-0002-7075-847X
Marc R. Dweck iD
https://orcid.org/0000-0001-9847-5917

Conflict of Interest
The authors have no financial conflicts of interest.

ABSTRACT

Aortic stenosis is the most common type of valvular heart disease. Aortic stenosis is characterized both by progressive valve narrowing and the left ventricular remodeling response that ensues. In aortic stenosis, therapeutic decision essentially depends on symptomatic status, stenosis severity, and status of left ventricular systolic function. Imaging is fundamental for the initial diagnostic work-up, follow-up, and selection of the optimal timing and type of intervention. Noninvasive imaging has played a pivotal role in enhancing our understanding of the complex pathophysiology underlying aortic stenosis, as well as disease progression in both the valve and myocardium. The present review provides the application of multimodality imaging in aortic stenosis.

Keywords: Aortic stenosis; Echocardiography; Dyspnea; Syncope; Angina; Diastolic dysfunction

INTRODUCTION

Aortic stenosis (AS) is a fibrocalcific disease in which deposition of lipid, collagen, and calcification leads to thickening and immobility of the aortic valve leaflets, resulting in progressive valve narrowing and obstruction to left ventricular outflow. Over time, the left ventricle (LV) responds to the consequent increase in afterload by myocyte hypertrophy, extracellular expansion, and ultimately myocardial fibrosis and decompensation.[1)2)]

In this review, we will discuss how modern advances in non-invasive imaging might optimize the assessment of AS and how the LV remodels in response to increased afterload. In particular, the established role of conventional echocardiography will be explored alongside emerging modalities such as speckle tracking echocardiography (STE), computed tomography (CT), cardiovascular magnetic resonance (CMR), and positron emission tomography (PET).

Generated by xmlinkpress

MULTIMODALITY IMAGING OF ASSESSMENT OF SEVERE AS

Transthoracic Doppler echocardiography

Echocardiography is considered the gold standard for cardiac clinical assessment. A comprehensive echocardiography report should contain information on aortic valve morphology (bicuspid versus tricuspid) and mobility, cause and severity of AS (including aortic valve area [AVA], mean gradient, and peak aortic jet velocity), and its consequences on LV function (i.e., stroke volume, LV ejection fraction [EF], and diastolic function), left atrial pressure, valvuloarterial impedance,[3] and pulmonary arterial pressure.[4]

Although multiple echocardiographic parameters are used to assess disease severity, current guidelines recommend the assessment of severity and prognosis be based on peak velocity, mean gradient, and AVA.[5][6] From a theoretical perspective, the ideal measurement for assessing AS severity has technical limitations. Potential limitations of echocardiography are also being increasingly described. First, acquisition of diagnostic acoustic windows can be impossible in certain patients, as can perfect alignment of the Doppler probe with the direction of maximal blood flow through the valve. In both circumstances, measurement errors will be introduced. Second, echocardiography may have difficulty in measuring the left ventricular outflow tract (LVOT) diameter with accuracy. Echocardiography often underestimates the LVOT diameter due to either calcification or its elliptical shape, and as the measurement is squared, small errors become substantially magnified. The continuity equation also relies on several geometric assumptions that frequently do not hold true in AS (such as a circular outflow tract and laminar flow profile), introducing further error. Therefore, LVOT diameter should be systematically reported to allow accurate monitoring of stenosis progression during follow-up. The LVOT diameter should be measured at the base of the aortic valve (AV) cusps or 1 to 5 mm below the aortic annulus using the zoomed view of the LVOT providing the largest diameter.

Multiple echocardiographic windows and a good Doppler alignment to the flow direction are used to detect the peak velocity (**Figure 1**). Peak velocity and mean gradient are dependent on flow status. AVA is in principle less flow-dependent. However, measurements of AVA can represent an important source of discrepancy, particularly as a result of variations in direct measurements of the LV outflow tract. These measurements can be challenging and rely on

| A | Apex | B | RPS |

AV Vmax = 3.5 m/sec
AV meanPG = 25.3 mmHg

AV Vmax = 5.1 m/sec
AV meanPG = 56.3 mmHg
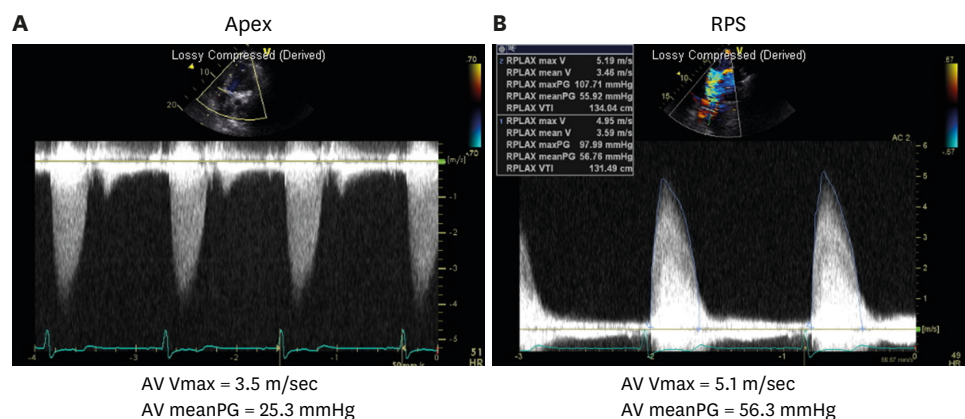
Figure 1. Continuous-wave Doppler recordings of aortic velocity in an elderly symptomatic patient with aortic stenosis. Peak velocities from the apex (Apex) (A) and right parasternal window (RPS) (B) are shown. Peak aortic valve velocity is higher (5.1 m/s) from the RPS position than from the apex (3.5 m/s). If continuous-wave Doppler had not been performed from the RPS position, the severity of aortic stenosis would have been underestimated.

the assumption that the LVOT is circular when it is in fact oval. As LV outflow tract diameter is squared to provide AVA by the continuity equation, small differences in measurement can lead to significant variation and often to an underestimation of AVA.[7] Discordant echocardiographic assessments of AS severity are therefore common and observed in around a quarter of patients with moderate or severe AS.[8]

Echocardiography can provide assessments of EF that are adequate for routine clinical use and are widely used for decision making. The current guidelines recommend AV replacement (AVR) in asymptomatic patients with severe AS if LVEF is less than 50%.[5][6] However recent data have suggested a higher threshold of 60% may be of greater clinical value. Ito et al.[9] demonstrated when patients with reduced LVEF at the time of initial diagnosis of severe AS were compared with those with preserved LVEF, LVEF was lower than 60% in the former group before AS became severe 5 to 10 years earlier, while the preserved LVEF group was found to have LVEF greater than 60%. The long-term prognosis of patients with an LVEF between 50% and 60% at the time of AVR was significantly lower than in patients with an LVEF greater than 60%.[9] Another registry from Japan involving 3,794 patients with severe AS also found higher mortality in patients with LVEF less than 60%.[10] These data suggest that an LVEF threshold of 60% may be of clinical utility, with further investigation required to assess whether patients with an LVEF below this cut-off do better with earlier AVR.

Low-dose (≤ 20 μg/kg per min) dobutamine echocardiography is recommended in low-flow, low-gradient AS with reduced LVEF (valve area < 1 cm^2, mean gradient < 40 mmHg, EF < 50%, stroke volume index ≤ 35 mL/m^2). In this setting to distinguish truly severe AS from pseudo-severe AS, which is defined by an increase to an AVA of > 1.0 cm^2 with flow normalization. In addition, the presence of a flow reserve (also termed contractile reserve; increase of stroke volume > 20%) has prognostic implications because it is associated with better outcomes.[6][11][12]

Diastolic function varies in patients with AS. Since patients with AS usually have left ventricular hypertrophy (LVH) and delayed myocardial relaxation, they usually have at least a mild degree (grade 1) of diastolic dysfunction. As AS progresses to symptoms, diastolic function also deteriorates to grades 2 and 3. Patients with severe AS and dyspnea were found to have higher E/e′ compared with others with chest pain or syncope.[13] Although current guidelines do not recommend the incorporation of diastolic function into management strategies for AS, our ability to manage patients with AS may be improved in the future if diastolic function is considered.

Transesophageal echocardiography

Transesophageal echocardiography (TEE) has the advantage of a higher spatial resolution. TEE is useful for grading AS severity in patients with poor transthoracic acoustic windows in whom the measurement of the LVOT diameter and anatomic or geometric AVA by planimetry is not feasible or inaccurate. While planimetry remains difficult on 2D imaging due to extensive calcification and difficulty ensuring position at the leaflet tips, it is more feasible on 3D TEE. Notably, however, planimetered AVAs do not exactly correspond to those measured using the continuity equation, so thresholds for severe disease are not clear. The measurement of effective AVA is also possible using the continuity equation provided that a good Doppler alignment to the aortic valve jet is achieved from the transgastric view. TEE can also be useful before transcatheter aortic valve implantation (TAVI) to evaluate the aortic annulus and the ascending aorta.
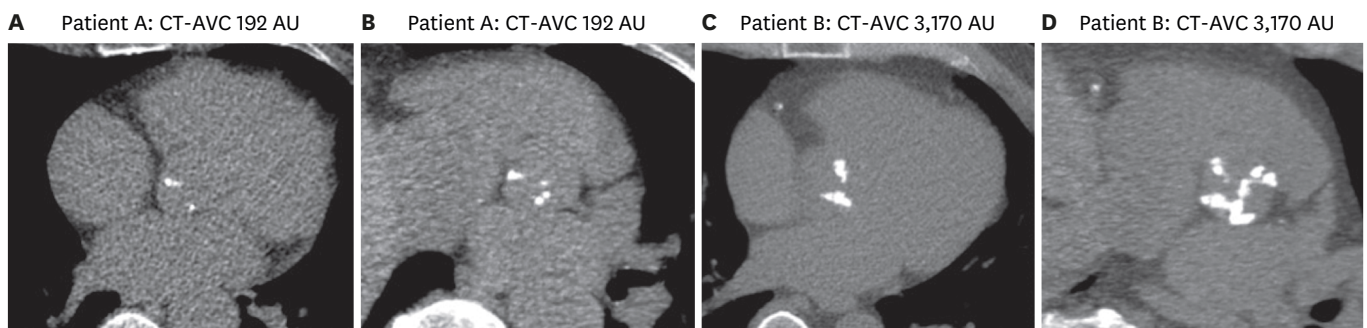
Speckle tacking echocardiography

Longitudinal LV motion is afterload-dependent and related to the presence of myocardial fibrosis. Global and longitudinal contraction of LV can be quantified by STE. Although echocardiography cannot directly assess myocardial fibrosis, LV global longitudinal strain (GLS) surrogate markers provide insights into the functional consequences of this fibrosis. Reduced GLS values have been correlated with the degree of myocardial fibrosis on cardiac magnetic resonance imaging[14] and histologic fibrosis.[15] In 688 patients with varying degrees of AS, GLS was found to be independently associated with all-cause mortality. GLS can further risk stratify AS patients and may influence the optimal timing of AVR.[16] GLS may provide prognostic information in asymptomatic severe AS while EF remains in the normal range.[17][18]

Computed tomography

Multislice computed tomography (MSCT) has a high spatial resolution and is particularly useful in patients with poor transthoracic acoustic windows or contraindications to TEE. Using 3-multiplanar reformations, from left sagittal oblique and left coronal oblique views, a cross-sectional view of the aortic valve can be generated for accurate measurement of anatomic AVA. A recent study showing asymmetrical LVOT by 3D imaging raised concerns about 2D echocardiographic AVA calculation accuracy but AVA calculation by multidetector CT (MDCT) does not improve grading concordance or outcome prediction.[19] There are differences between echocardiography and CT measurements, but echocardiography-measured AVA is not inferior to that calculated using LVOT by MDCT. Thus, measurement of LVOT diameter by MDCT is a valuable method to calculate AVA to assess AS severity. However, the use of MDCT is not mandatory in clinical routine for the evaluation of AS severity, and echocardiography should remain the first-line evaluation strategy. Nevertheless, MDCT may be helpful in patients in whom there is a doubt about the aortic annulus diameter measurements by echocardiography for any reason.

MSCT allows accurate measurement of aortic annulus diameters (sagittal + coronal + mean values), area, and perimeter, which are key parameters for the selection of the prosthesis size before TAVI.

Calcification is the predominant process causing valve obstruction in AS. Quantification of the calcium burden has therefore been suggested as an alternative flow-independent method for determining disease severity.[20] Calcium burden in the AV can be accurately quantified on electrocardiography-gated non-contrast CT. Indeed, CT-AV calcium scoring (CT-AVC) can then be measured using the same protocols as coronary calcium scoring and the Agatston score (AU), which accounts for both the density and volume of CT-measured calcium and correlates closely with the weight of calcium in explanted aortic valves (**Figure 2**).[21] Recently,

A Patient A: CT-AVC 192 AU **B** Patient A: CT-AVC 192 AU **C** Patient B: CT-AVC 3,170 AU **D** Patient B: CT-AVC 3,170 AU

Figure 2. CT calcium scoring in the aortic valve. An example of mild AVC of Patient A (A, B) and severe calcification by CT of Patient B in axial (C) and short-axis (D) views of the valve. Reproduced with permission from Dweck et al.[50] AU: arbitrary unit(s), AVC: aortic valve calcification, CT: computed tomography.

sex-specific cut offs for severe AS (women 1,300 AU, men 2,000 AU) have been proposed and validated in large international multi-center studies, demonstrating excellent diagnostic accuracy compared with echocardiography and powerful prediction of clinical outcomes.[8)21-25] CT-AVC is now recommended in the European Society of Cardiology Guidelines as an arbitrator of AS severity when echocardiographic assessments are discordant.[6]

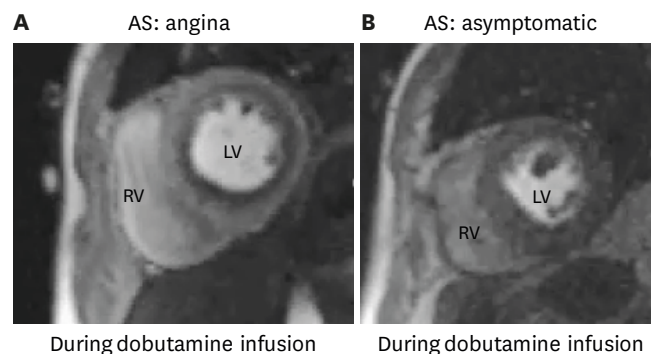# CARDIOVASCULAR MAGNETIC RESONANCE

Adenosine-stress CMR

Myocardial ischemia in patients with severe AS can occur in the absence of coronary artery disease (CAD) and appears to be due to inadequate LVH with high systolic and diastolic wall stresses and a somewhat reduced coronary flow reserve.

In the absence of significant coronary stenosis, this finding is indicative of microvascular dysfunction, but whether the reduced myocardial perfusion reserve seen in severe AS without obstructive CAD leads to angina during stress stimuli remains unclear.

Adenosine-stress CMR can detect stress-induced abnormal hypoperfusion with signs and symptoms of ischemia without CAD.[26)27] This is almost the only noninvasive clinical method that allows assessment of the transmyocardial distribution of coronary blood flow and myocardial perfusion reserve index. A previous study by Ahn et al.[28] in severe AS patients with angina but no obstructive CAD demonstrated a reduced myocardial perfusion reserve, which is indicative of microvascular dysfunction, compared with severe AS patients without any symptoms (**Figure 3**). Ahn et al.[28] suggests that angina in patients with severe AS without obstructive CAD might be attributed to LVH, which can cause myocardial ischemia by coronary microvascular dysfunction.

Strain imaging on CMR

Strain imaging on CMR can be a valuable noninvasive tool to evaluate and quantify myocardial deformation before any identifiable changes in EF. CMR myocardial tissue tracking on steady-state free precession (SSFP) cine-imaging has been developed to satisfy the needs for fast and quantitative assessment of myocardial segmental and global strain analysis.[29)30] CMR tissue tracking is the recently developed CMR-equivalent of STE.[29] CMR

A AS: angina   **B** AS: asymptomatic

LV, RV (panel A); LV, RV (panel B)

During dobutamine infusion   During dobutamine infusion

Figure 3. Representative images from adenosine-stress CMR in the angina and asymptomatic groups. (A) Representative adenosine stress perfusion image from the angina group: perfusion defect seen during adenosine infusion (low signal intensity area). (B) Representative adenosine stress perfusion image from the asymptomatic group: no evidence of inducible perfusion defect. AS: aortic stenosis, CMR: cardiovascular magnetic resonance, LV: left ventricle, RV: right ventricle.

tissue tracking has been validated against myocardial tagging.[31-33] Importantly, CMR tissue tracking can be undertaken using SSFP imaging, which is part of a routine CMR scan, and no additional sequences are required.[34] Hwang et al.[35] demonstrated that longitudinal global strain measured by CMR tissue tracking correlated with reverse remodeling as LV mass index regressed and was predictive of this outcome (**Figure 4**). As a simple and practical method, tissue tracking is promising to assess strain and predict reverse remodeling in severe AS, especially in patients with suboptimal echocardiography image quality.[35]

### Late gadolinium enhancement and T1 mapping techniques

The major strength of CMR is its ability to provide noninvasive myocardial tissue characterization using late gadolinium enhancement (LGE) and T1 mapping techniques.

LGE is the most studied and best validated imaging method for detecting myocardial fibrosis in AS. Non-infarct (or mid-wall) LGE is associated with poor long-term outcomes. Previous studies have demonstrated non-infarct LGE to be an independent predictor of mortality, of incremental value to valve assessments, and LVEF.[36-41] The EVOLVED (Early Valve Replacement Guided by Biomarkers of Left Ventricular Decompensation in Asymptomatic Patients with Severe Aortic Stenosis) randomized controlled trial is investigating whether early AVR in asymptomatic patients with non-infarct LGE improves long-term patient outcomes (NCT03094143).

Myocardial fibrosis may also be present in a diffuse interstitial pattern, which is not detected by LGE techniques. Instead, this process may be identified and quantified using T1 mapping techniques that estimate absolute T1 values in a voxel-by-voxel map. Correlations between native T1 and both the degree of diffuse fibrosis on histology and the extent of ventricular remodeling on CMR have been demonstrated.[42)43] Recently, Lee et al.[44] showed that native T1 was an independent predictor of heart failure hospitalization or death (2.4% vs. 11.6% vs. 42.9% for low, mid, and high tertiles of native T1, respectively; $p < 0.001$) in 127 patients with moderate or severe AS. Although native T1 is relatively uniform and reproducible when using the same sequence and scanner on the same patient, values are subject to a variety of factors such as patient age and sex, acquisition sequence, scanner field strength, and post-processing.[45]

T1 mapping can also be repeated following administration of gadolinium, which enables calculation of the extracellular volume fraction (ECV%) (i.e., the fraction of the myocardial volume that is extracellular space). ECV% has been investigated as a method for detecting diffuse myocardial fibrosis in AS. A number of clinical studies have validated ECV% against histology in AS and have demonstrated the association between ECV% and other markers of LV decompensation, including ECG changes in hypertrophy and strain, and elevation in biomarkers, such as troponin and N-terminal pro-brain natriuretic peptide.[38)46)47] Data on the prognostic value of ECV% in AS are limited. Recently, Park et al.[15] demonstrated that ECV% ($r = 0.465$, $p < 0.0001$), GLS ($r = 0.421$, $p = 0.0003$), and native T1 value ($r = 0.429$, $p = 0.0002$) were significantly correlated with the degree of histologic myocardial fibrosis in 71 consecutive patients with severe AS. ECV% was more closely related to prediction of the clinical outcome than native T1 or GLS in those patients (**Figure 5**).

Whereas ECV% provides a percentage estimate, the indexed extracellular volume (iECV) provides an assessment of the total fibrosis burden in the myocardium. iECV is calculated by multiplying ECV% by the indexed left ventricular myocardial volume: iECV = ECV% × indexed
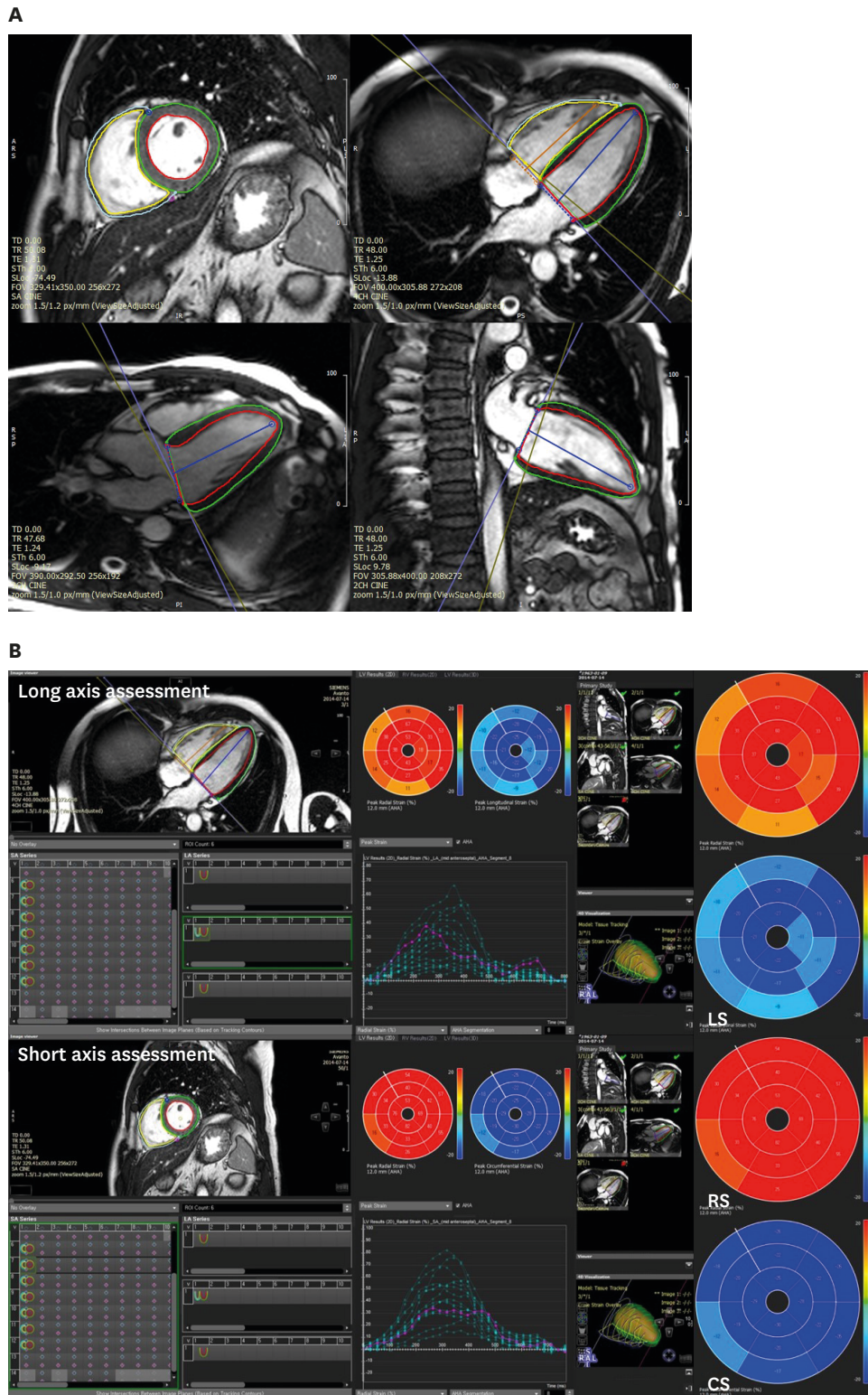
Figure 4. CMR myocardial tissue tracking analysis. (A) CMR tissue tracking analyses were performed using commercially available software (cvi42 version 5, Circle Cardiovascular Imaging Inc., Calgary, Alberta, Canada). (B) Two-, three-, and four-chamber, and short axis images were uploaded into the software, which reconstructs a 3D model that is used for analyses of 2D- and 3D radial, circumferential and longitudinal LV strain. CMR: cardiovascular magnetic resonance, LV: left ventricle, RV: right ventricle.
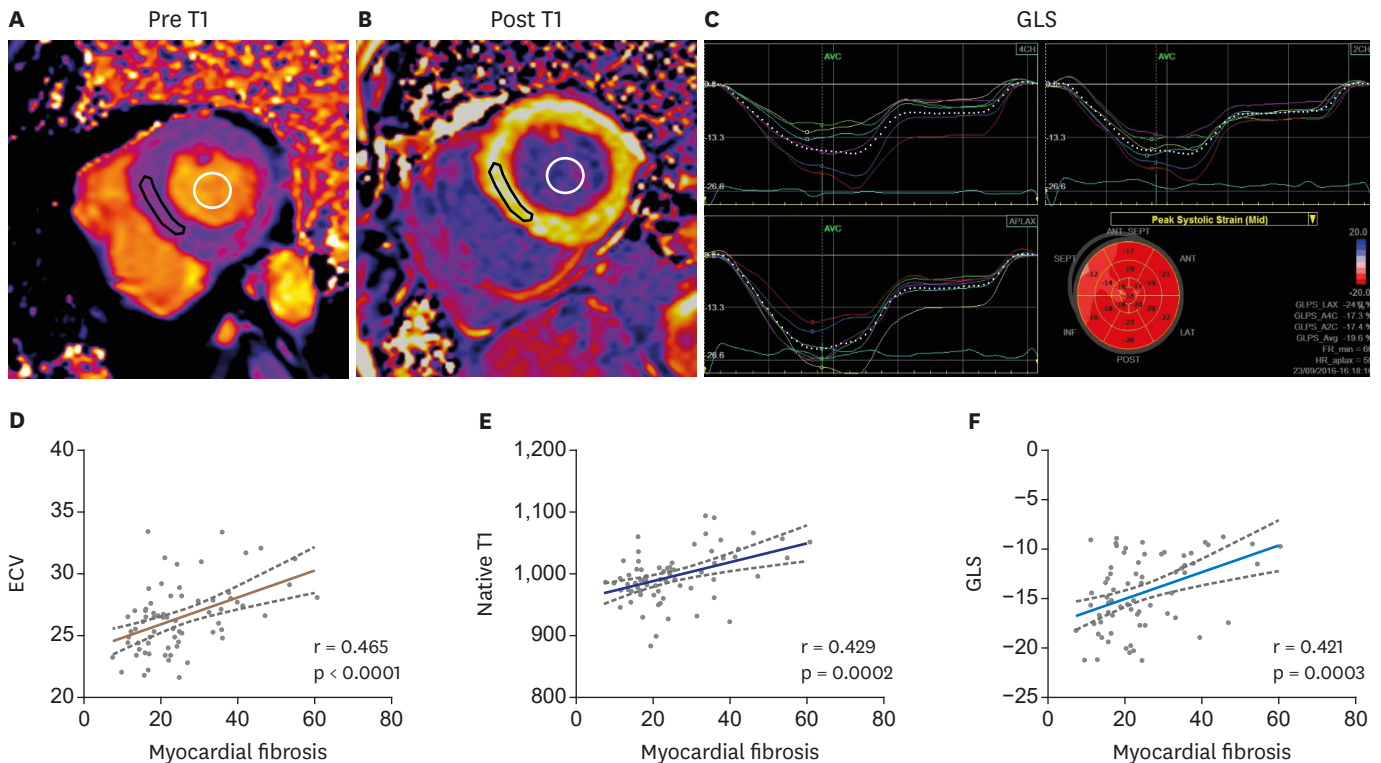
Figure 5. Measurement of T1 mapping in CMR and GLS in STE. Pre T1 (A) and post T1 (B) mapping images, the ROI was drawn manually at the basal septum (dark line) and LV cavity (white line) for native T1 value and ECV. (C) GLS in STE. GLS was acquired by average regional strain curves (16-segment model for 2D STE). Correlation between MF and ECV (D), native T1 value (E), and GLS (F). The ECV (r = 0.465, p < 0.0001), GLS (r = 0.421, p = 0.0003), and native T1 value (r = 0.429, p = 0.0002) were significantly correlated with the degree of MF. CMR: cardiovascular magnetic resonance, ECV: extracellular volume fraction, GLS: global longitudinal strain, MF: myocardial fibrosis, ROI: region of interest, STE: speckle tracking echocardiography.

left ventricular myocardial volume.[38] iECV and ECV% have recently been used in combination to study changes in the composition of the intracellular and extracellular compartments before and after AVR.[48][49]

Positron emission tomography

PET is another novel technique that is being explored for use in AS. Radiolabeled sodium fluoride (^{18}F-NaF) is a widely available PET tracer that exchanges with hydroxyl groups on hydroxyapatite crystals, a key structural component of both bone and vascular calcification. PET can be used to measure calcification activity in the vasculature, with an affinity for areas of developing microcalcification.[50][51] Previous studies have shown that ^{18}F-NaF activity is increased in patients with AV disease compared with the healthy population, with a progressive rise in PET uptake with increasing severity of AS.[52] Furthermore, ^{18}F-NaF activity predicts the rate of future disease progression as measured by CT-AVC and echocardiography.[50][53] Indeed, new areas of macrocalcification appear to subsequently develop at sites of increased baseline ^{18}F-NaF uptake, consistent with this tracer identifying developing calcification before it is visible on CT (**Figure 6**).[50] Although the expense and availability of PET may limit future widespread clinical application, ^{18}F-fluoride PET is increasingly being used as an endpoint in clinical trials evaluating the efficacy of novel therapies in AS (e.g., SALTIRE II [Study Investigating the Effects of Drugs Used to Treat Osteoporosis on the Progression of Calcific Aortic Stenosis] NCT02132026, BASIK 2 [Bicuspid Aortic Valve Stenosis and the Effect of Vitamin K2 on Calcium Metabolism on ^{18}F-NaF PET/MRI] NCT02917525).

A Patient 1
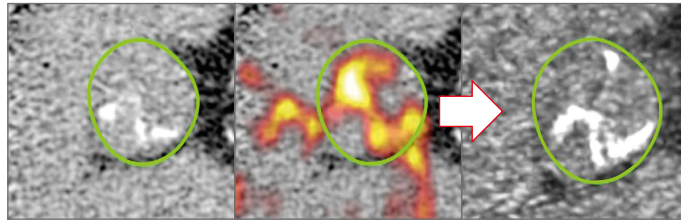
B Patient 2
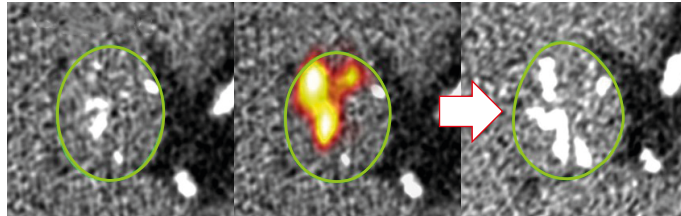
Figure 6. ^{18}F-NaF PET-CT predicts disease progression in AS. Baseline CT calcium score scans (left) for patients 1 (A) and 2 (B). Fused ^{18}F-NaF PET-CT scans (middle) show fluoride uptake in red and yellow. Follow-up CT at 1 year (right) suggests that the baseline PET signal predicts where new macroscopic calcium, visible on the CT, is going to develop. Reproduced with permission from Dweck et al.[50] ^{18}F-NaF: radiolabeled sodium fluoride, CT: computed tomography, PET: positron emission tomography.

CONCLUSION

Although echocardiographic assessments remain the clinical gold standard in AS and are used widely to guide patient management, multi-modality imaging approaches including CT calcium scoring, CMR, and ^{18}F-NaF PET imaging are being used to assess disease activity and disease progression, improve patient risk stratification, assess novel treatments, and potentially optimize the timing of AV interventions.

REFERENCES

1. Pawade TA, Newby DE, Dweck MR. Calcification in aortic stenosis: the skeleton key. *J Am Coll Cardiol* 2015;66:561-77.
   PUBMED | **CROSSREF**

2. Dweck MR, Boon NA, Newby DE. Calcific aortic stenosis: a disease of the valve and the myocardium. *J Am Coll Cardiol* 2012;60:1854-63.
   PUBMED | **CROSSREF**

3. Jang JY, Seo JS, Sun BJ, et al. Impact of valvuloarterial impedance on concentric remodeling in aortic stenosis and its regression after valve replacement. *J Cardiovasc Ultrasound* 2016;24:201-7.
   PUBMED | **CROSSREF**

4. Dulgheru R, Pibarot P, Sengupta PP, et al. Multimodality imaging strategies for the assessment of aortic stenosis: viewpoint of the Heart Valve Clinic International Database (HAVEC) group. *Circ Cardiovasc Imaging* 2016;9:e004352.
   PUBMED | **CROSSREF**

5. Nishimura RA, Otto CM, Bonow RO, et al. 2017 AHA/ACC focused update of the 2014 AHA/ACC guideline for the management of patients with valvular heart disease: a report of the American College of Cardiology/American Heart Association Task Force on Clinical Practice Guidelines. *J Am Coll Cardiol* 2017;70:252-89.
   PUBMED | **CROSSREF**

6. Baumgartner H, Falk V, Bax JJ, et al. 2017 ESC/EACTS Guidelines for the management of valvular heart disease. *Eur Heart J* 2017;38:2739-91.
   PUBMED | **CROSSREF**

7. Doris MK, Everett RJ, Shun-Shin M, Clavel MA, Dweck MR. The role of imaging in measuring disease progression and assessing novel therapies in aortic stenosis. *JACC Cardiovasc Imaging* 2019;12:185-97.
    PUBMED | CROSSREF

8. Clavel MA, Messika-Zeitoun D, Pibarot P, et al. The complex nature of discordant severe calcified aortic valve disease grading: new insights from combined Doppler echocardiographic and computed tomographic study. *J Am Coll Cardiol* 2013;62:2329-38.
    PUBMED | CROSSREF

9. Ito S, Miranda WR, Nkomo VT, et al. Reduced left ventricular ejection fraction in patients with aortic stenosis. *J Am Coll Cardiol* 2018;71:1313-21.
    PUBMED | CROSSREF

10. Taniguchi T, Morimoto T, Shiomi H, et al. Prognostic impact of left ventricular ejection fraction in patients with severe aortic stenosis. *JACC Cardiovasc Interv* 2018;11:145-57.
    PUBMED | CROSSREF

11. Monin JL, Quéré JP, Monchi M, et al. Low-gradient aortic stenosis: operative risk stratification and predictors for long-term outcome: a multicenter study using dobutamine stress hemodynamics. *Circulation* 2003;108:319-24.
    PUBMED | CROSSREF

12. Levy F, Laurent M, Monin JL, et al. Aortic valve replacement for low-flow/low-gradient aortic stenosis operative risk stratification and long-term outcome: a European multicenter study. *J Am Coll Cardiol* 2008;51:1466-72.
    PUBMED | CROSSREF

13. Park SJ, Enriquez-Sarano M, Chang SA, et al. Hemodynamic patterns for symptomatic presentations of severe aortic stenosis. *JACC Cardiovasc Imaging* 2013;6:137-46.
    PUBMED | CROSSREF

14. Ng ACT, Prihadi EA, Antoni ML, et al. Left ventricular global longitudinal strain is predictive of all-cause mortality independent of aortic stenosis severity and ejection fraction. *Eur Heart J Cardiovasc Imaging* 2018;19:859-67.
    PUBMED | CROSSREF

15. Park SJ, Cho SW, Kim SM, et al. Assessment of myocardial fibrosis using multimodality imaging in severe aortic stenosis: comparison with histologic fibrosis. *JACC Cardiovasc Imaging* 2019;12:109-19.
    PUBMED | CROSSREF

16. Salaun E, Casalta AC, Donal E, et al. Apical four-chamber longitudinal left ventricular strain in patients with aortic stenosis and preserved left ventricular ejection fraction: analysis related with flow/gradient pattern and association with outcome. *Eur Heart J Cardiovasc Imaging* 2018;19:868-78.
    PUBMED | CROSSREF

17. Lancellotti P, Magne J, Dulgheru R, et al. Outcomes of patients with asymptomatic aortic stenosis followed up in heart valve clinics. *JAMA Cardiol* 2018;3:1060-8.
    PUBMED | CROSSREF

18. Vollema EM, Sugimoto T, Shen M, et al. Association of left ventricular global longitudinal strain with asymptomatic severe aortic stenosis: natural course and prognostic value. *JAMA Cardiol* 2018;3:839-47.
    PUBMED | CROSSREF

19. Clavel MA, Malouf J, Messika-Zeitoun D, Araoz PA, Michelena HI, Enriquez-Sarano M. Aortic valve area calculation in aortic stenosis by CT and Doppler echocardiography. *JACC Cardiovasc Imaging* 2015;8:248-57.
    PUBMED | CROSSREF

20. Rosenhek R, Binder T, Porenta G, et al. Predictors of outcome in severe, asymptomatic aortic stenosis. *N Engl J Med* 2000;343:611-7.
    PUBMED | CROSSREF

21. Messika-Zeitoun D, Aubry MC, Detaint D, et al. Evaluation and clinical implications of aortic valve calcification measured by electron-beam computed tomography. *Circulation* 2004;110:356-62.
    PUBMED | CROSSREF

22. Cueff C, Serfaty JM, Cimadevilla C, et al. Measurement of aortic valve calcification using multislice computed tomography: correlation with haemodynamic severity of aortic stenosis and clinical implication for patients with low ejection fraction. *Heart* 2011;97:721-6.
    PUBMED | CROSSREF

23. Clavel MA, Pibarot P, Messika-Zeitoun D, et al. Impact of aortic valve calcification, as measured by MDCT, on survival in patients with aortic stenosis: results of an international registry study. *J Am Coll Cardiol* 2014;64:1202-13.
    PUBMED | CROSSREF

24. Pawade T, Clavel MA, Tribouilloy C, et al. Computed tomography aortic valve calcium scoring in patients with aortic stenosis. *Circ Cardiovasc Imaging* 2018;11:e007146.
    PUBMED | CROSSREF

25. Tastet L, Enriquez-Sarano M, Capoulade R, et al. Impact of aortic valve calcification and sex on hemodynamic progression and clinical outcomes in AS. *J Am Coll Cardiol* 2017;69:2096-8.
PUBMED | CROSSREF

26. Panting JR, Gatehouse PD, Yang GZ, et al. Abnormal subendocardial perfusion in cardiac syndrome X detected by cardiovascular magnetic resonance imaging. *N Engl J Med* 2002;346:1948-53.
PUBMED | CROSSREF

27. Lanza GA, Buffon A, Sestito A, et al. Relation between stress-induced myocardial perfusion defects on cardiovascular magnetic resonance and coronary microvascular dysfunction in patients with cardiac syndrome X. *J Am Coll Cardiol* 2008;51:466-72.
PUBMED | CROSSREF

28. Ahn JH, Kim SM, Park SJ, et al. Coronary microvascular dysfunction as a mechanism of angina in severe AS: prospective adenosine-stress CMR study. *J Am Coll Cardiol* 2016;67:1412-22.
PUBMED | CROSSREF

29. Hor KN, Baumann R, Pedrizzetti G, et al. Magnetic resonance derived myocardial strain assessment using feature tracking. *J Vis Exp* 2011:2356.
PUBMED

30. Maret E, Todt T, Brudin L, et al. Functional measurements based on feature tracking of cine magnetic resonance images identify left ventricular segments with myocardial scar. *Cardiovasc Ultrasound* 2009;7:53.
PUBMED | CROSSREF

31. Harrild DM, Han Y, Geva T, Zhou J, Marcus E, Powell AJ. Comparison of cardiac MRI tissue tracking and myocardial tagging for assessment of regional ventricular strain. *Int J Cardiovasc Imaging* 2012;28:2009-18.
PUBMED | CROSSREF

32. Schneeweis C, Lapinskas T, Schnackenburg B, et al. Comparison of myocardial tagging and feature tracking in patients with severe aortic stenosis. *J Heart Valve Dis* 2014.23:432-40.
PUBMED

33. Hor KN, Gottliebson WM, Carson C, et al. Comparison of magnetic resonance feature tracking for strain calculation with harmonic phase imaging analysis. *JACC Cardiovasc Imaging* 2010;3:144-51.
PUBMED | CROSSREF

34. Wu L, Germans T, Güçlü A, Heymans MW, Allaart CP, van Rossum AC. Feature tracking compared with tissue tagging measurements of segmental strain by cardiovascular magnetic resonance. *J Cardiovasc Magn Reson* 2014;16:10.
PUBMED | CROSSREF

35. Hwang JW, Kim SM, Park SJ, et al. Assessment of reverse remodeling predicted by myocardial deformation on tissue tracking in patients with severe aortic stenosis: a cardiovascular magnetic resonance imaging study. *J Cardiovasc Magn Reson* 2017;19:80.
PUBMED | CROSSREF

36. Azevedo CF, Nigri M, Higuchi ML, et al. Prognostic significance of myocardial fibrosis quantification by histopathology and magnetic resonance imaging in patients with severe aortic valve disease. *J Am Coll Cardiol* 2010;56:278-87.
PUBMED | CROSSREF

37. Aquaro GD, Perfetti M, Camastra G, et al. Cardiac MR with late gadolinium enhancement in acute myocarditis with preserved systolic function: ITAMY study. *J Am Coll Cardiol* 2017;70:1977-87.
PUBMED | CROSSREF

38. Chin CWL, Everett RJ, Kwiecinski J, et al. Myocardial fibrosis and cardiac decompensation in aortic stenosis. *JACC Cardiovasc Imaging* 2017;10:1320-33.
PUBMED | CROSSREF

39. Halliday BP, Gulati A, Ali A, et al. Association between midwall late gadolinium enhancement and sudden cardiac death in patients with dilated cardiomyopathy and mild and moderate left ventricular systolic dysfunction. *Circulation* 2017;135:2106-15.
PUBMED | CROSSREF

40. Musa TA, Treibel TA, Vassiliou VS, et al. Myocardial scar and mortality in severe aortic stenosis. *Circulation* 2018;138:1935-47.
PUBMED | CROSSREF

41. Dweck MR, Joshi S, Murigu T, et al. Midwall fibrosis is an independent predictor of mortality in patients with aortic stenosis. *J Am Coll Cardiol* 2011;58:1271-9.
PUBMED | CROSSREF

42. Bull S, White SK, Piechnik SK, et al. Human non-contrast T1 values and correlation with histology in diffuse fibrosis. *Heart* 2013;99:932-7.
PUBMED | CROSSREF

43. Lee SP, Lee W, Lee JM, et al. Assessment of diffuse myocardial fibrosis by using MR imaging in asymptomatic patients with aortic stenosis. *Radiology* 2015;274:359-69.
    PUBMED | CROSSREF

44. Lee H, Park JB, Yoon YE, et al. Noncontrast myocardial T1 mapping by cardiac magnetic resonance predicts outcome in patients with aortic stenosis. *JACC Cardiovasc Imaging* 2018;11:974-83.
    PUBMED | CROSSREF

45. Bing R, Cavalcante JL, Everett RJ, Clavel MA, Newby DE, Dweck MR. Imaging and impact of myocardial fibrosis in aortic stenosis. *JACC Cardiovasc Imaging* 2019;12:283-96.
    PUBMED | CROSSREF

46. Treibel TA, López B, González A, et al. Reappraising myocardial fibrosis in severe aortic stenosis: an invasive and non-invasive study in 133 patients. *Eur Heart J* 2018;39:699-709.
    PUBMED | CROSSREF

47. Chin CW, Shah AS, McAllister DA, et al. High-sensitivity troponin I concentrations are a marker of an advanced hypertrophic response and adverse outcomes in patients with aortic stenosis. *Eur Heart J* 2014;35:2312-21.
    PUBMED | CROSSREF

48. Treibel TA, Kozor R, Schofield R, et al. Reverse myocardial remodeling following valve replacement in patients with aortic stenosis. *J Am Coll Cardiol* 2018;71:860-71.
    PUBMED | CROSSREF

49. Everett RJ, Tastet L, Clavel MA, et al. Progression of hypertrophy and myocardial fibrosis in aortic stenosis: a multicenter cardiac magnetic resonance study. *Circ Cardiovasc Imaging* 2018;11:e007451.
    PUBMED | CROSSREF

50. Dweck MR, Jenkins WS, Vesey AT, et al. 18F-sodium fluoride uptake is a marker of active calcification and disease progression in patients with aortic stenosis. *Circ Cardiovasc Imaging* 2014;7:371-8.
    PUBMED | CROSSREF

51. Joshi NV, Vesey AT, Williams MC, et al. 18F-fluoride positron emission tomography for identification of ruptured and high-risk coronary atherosclerotic plaques: a prospective clinical trial. *Lancet* 2014;383:705-13.
    PUBMED | CROSSREF

52. Aggarwal SR, Clavel MA, Messika-Zeitoun D, et al. Sex differences in aortic valve calcification measured by multidetector computed tomography in aortic stenosis. *Circ Cardiovasc Imaging* 2013;6:40-7.
    PUBMED | CROSSREF

53. Jenkins WS, Vesey AT, Shah AS, et al. Valvular (18)F-fluoride and (18)F-fluorodeoxyglucose uptake predict disease progression and clinical outcome in patients with aortic stenosis. *J Am Coll Cardiol* 2015;66:1200-1.
    PUBMED | CROSSREF